Available online at www.sciencedirect.com
SCIENCE DIRECT
Polymer 46 (2005) 4654–4663
polymer
www.elsevier.com/locate/polymer

# Synthesis, optical and morphological characterization of soluble main chain 1,3,4-oxadiazole copolyarylethers—potential candidates for solar cells applications as electron acceptors

Christos L. Chochos[a,b], Giannis K. Govaris[a,c], Fotini Kakali[b], Panagiotis Yiannoulis[c], Joannis K. Kallitsis[a,b], Vasilis G. Gregoriou[a,*]

[a]*Foundation for Research and Technology Hellas (FORTH-ICEHT), Institute of Chemical Engineering and High Temperature Processes, P.O. Box 1414, 26500 Patras, Greece*
[b]*Department of Chemistry, University of Patras, 26500 Patras, Greece*
[c]*Department of Physics, University of Patras, 26500 Patras, Greece*

Received 30 July 2004; received in revised form 15 March 2005; accepted 22 March 2005
Available online 21 April 2005

**Abstract**

New copoly(arylether)s containing substituted terphenyl, quinquephenyl, fluorene and anthracene moieties with aromatic 1,3,4-oxadiazole units were prepared and the resulting copolymers are soluble in common organic solvents. Investigation of their optical properties revealed that they emit blue and yellow light. Moreover, their photovoltaic response was studied in blends with poly(3-hexylthiophene) (P3HT) as the electron donor. Despite the low power conversion efficiencies it was shown that photo-induced electron transfer does take place and the performances are higher than a single layer P3HT device. In addition, an anthracene–fluorene–oxadiazole main chain copolymer (PAFOXD) was also examined in a single layer photovoltaic device and gave one of the highest reported open-circuit voltage ($V_{oc}$) values in the literature (0.89 V). Finally, a detailed morphological study of the blends and the PAFOXD surface using the atomic force microscopy (AFM) technique, revealed the effect of solvent selection to the preparation of thin films exhibiting the desired performance characteristics.


*Keywords:* Soluble main chain oxadiazoles; High open-circuit voltage; Solar cells

## 1. Introduction

Solar energy offers great potential as a renewable source for conversion to electrical power. The demand for renewable energy sources is the driving force behind new approaches in the development of low-cost photovoltaic devices. The prospect of roll-to-roll processing makes organic semiconducting materials intriguing alternatives for future generations of photovoltaic devices [1]. However, power conversion efficiencies are not yet high enough for organic based devices to be commercially viable. An encouraging breakthrough in realizing higher efficiencies has been achieved by mixing electron donor type polymers with suitable electron acceptors. Efficient organic solar cells have been developed based on the bulk heterojunction concept of a conjugated polymer and a soluble derivative of the fullerene ($C_{60}$ or $C_{70}$, PCBM) with power conversion efficiencies of approximately 3% [2]. The power conversion efficiency is determined, in part, by the short-circuit current and the open-circuit voltage of the device. Improvement of the energy conversion efficiency of these devices relies on optimizing: (1) the charge carrier generation; (2) the selective transport and collection of charges at the electrodes; (3) the absorption of light.

The photovoltaic effect involves the generation of electron and hole pairs and their subsequent collection at the opposite electrodes. Studying photovoltaic efficiency in relation to morphology and mesoscopic ordering in the active layer is of intense interest [3]. One of the factors that plays an important role is the low entropy of mixing between two polymers. When a polymer blend is spin-coated from a well-mixed solution, the faster the solvent

* Corresponding author. Tel.: +30 2610 965205; fax: +30 2610 965223.
*E-mail address:* gregoriou@iceht.forth.gr (V.G. Gregoriou).

0032-3861/$ - see front matter © 2005 Elsevier Ltd. All rights reserved.
doi:10.1016/j.polymer.2005.03.080

evaporates, the less time the polymer has to rearrange itself into discrete domains. Phase separation is then taking place and domain sizes of a few nanometers to several microns are created. By controlling the morphology of the phase separation into an interpenetrating bi-continuous network of donor and acceptor phases on a nanoscopic scale (~10 nm), one can achieve a high interfacial area within a bulk heterojunction blend. However, the actual charge collection efficiency has not reach yet such values that will enable the commercialization of the device because the perfect charge transfer reaction is only effective at the interface, not in the bulk. The development of certain techniques such as annealing the film after spin-coating, exposure it to solvent vapors or controlling the rate of solvent evaporation could alter the morphology of the blend and a phase separation on the scale of ~10 nm can be achieved.

Charge transport efficiency is an essential parameter capable of improving the performance of such optoelectronic devices. Well known hole transport (p-type) conjugated polymers are the poly(*p*-phenylenevinylene)s (PPVs), poly(*p*-phenylene)s, polythiophenes as well as their derivates. Poly(3-hexylthiophene) (P3HT) is one of the best candidates due to low energy band gap suitable for red light absorption, the high charge carrier mobility and the excellent solubility in organic solvents. In addition, electron accepting optoelectronic materials (n-type) with high electron affinity have recently been synthesized and investigated. Main chain polyquinoxalines, [4] polyquinolines [5] and main chain as well as side chain polyoxadiazoles [6] are representative class of materials which combine the high electron affinity with high thermal and oxidative stability, outstanding mechanical properties and good film-forming ability [7]. Furthermore several oxadiazole-containing polymers have been employed as electron transporting materials in organic light emitting diodes (OLEDs) [8]. This ability to carry electrons is believed to arise from the high electron affinity of the oxadiazole ring in the molecule. However, due to their low solubility, these compounds possess poor solution processability. Therefore, a lot of effort has been consumed to incorporate π-conjugated oligomers into polymers either as polymer backbones or as side chains in order to improve their solubility [9].

In this work, we present the synthesis of four new main chain 1,3,4-oxadiazole copolyethers (**I–IV**) by the nucleophilic polycondensation reaction and their optical characterization. Moreover, a fluorene copolymer containing 1,3,4-oxadiazole unit (PFOXD) was also synthesized by Suzuki coupling reaction. In addition, a detailed AFM study of the surface morphology of the blends consisted of the regioregular poly(3-hexyl)thiophene with TSTPOXD and PFOXD as thin films was performed. Finally, the photovoltaic response of the TSTPOXD or PFOXD with the P3HT as bulk heterojunction mixtures and a single layer device of the PAFOXD were investigated.

## 2. Experimental section

### 2.1. Materials and measurements

Regioregular poly(3-hexylthiophene) (P3HT) was received from Aldrich and all the other chemicals and solvents were purchased from Aldrich or Acros and used without purification unless otherwise noted. TSTDIOL, TSQDIOL, ANTDIOL, and (FPh)2OXD were prepared according to literature procedures (Schemes 1 and 2) [10]. The structures of the synthesized monomers (FLUDIOL and (BrPh)2OXD) as well as the soluble oxadiazole polyethers were clarified by high-resolution $^1$H NMR spectroscopy with a Bruker Avance DPX 400 MHz spectrometer (Fig. 1). Molecular weights ($M_n$ and $M_w$) were determined by gel permeation chromatography (Ultrastyragel columns with 500 and $10^4$ Å pore size; $CHCl_3$ (analytical grade) was filtered through a 0.2 μm millipore filter; flow 1 mL min$^{-1}$; room temperature) using polystyrene standards for calibration. The UV spectra were recorded on a Hewlett Packard 8452A Diode Array UV–visible Spectrophotometer. Fluorescence spectra were measured on a Perkin–Elmer LS50B spectrofluorimeter. Photovoltaic devices were prepared according to the following procedure: the indium tin oxide (ITO) coated glass substrate, purchased from Merck, with a surface resistance of 15 Ω/square, was first cleaned by ultrasonication in organic solvents. Afterwards it was coated with a film of poly(3,4-ethylenedioxythiophene)–poly(styrenesulfonate) (PEDOT–PSS) in aqueous solution, purchased from Bayer AG, using spin-casting technology. The thickness of PEDOT–PSS layer was approximately 100 nm. After the PEDOT film had dried overnight, the photoactive layer was casted on the top of the PEDOT layer by spin-coating resulting in approximately 100 nm thickness. Spin-coating conditions were kept the same both for PEDOT and active layer deposition: initial spinning speed was 1500 rpm for 60 s followed by 3000 rpm for 60 s. The aluminum (Al) top electrode, which typically had a thickness of about 100 nm, was deposited by means of thermal evaporation in vacuum better than $10^{-5}$ mbar onto the organic layer, resulting in the device architecture depicted in Scheme 3. The size of the active area of the solar cell, as defined by the Al back electrode, was 4 mm$^2$. Current–voltage curves were measured with a Kiethley SMU 236 unit under an illumination intensity of 50 mW cm$^{-2}$ in a home made solar simulator simulating the AM1.5 sun spectrum. Illumination occurred through the transparent ITO side. All fabrication steps and *I–V* measurements were carried out in normal lab atmosphere. Imaging of the surface morphology of spin-coated samples was accomplished via AFM. A Topometrix Explorer SPM Microscope (theromicroscopes) equipped with a scanner of maximum ranges of 100 and 10 μm in *xy* and *z* directions, respectively, was used for the AFM measurements.

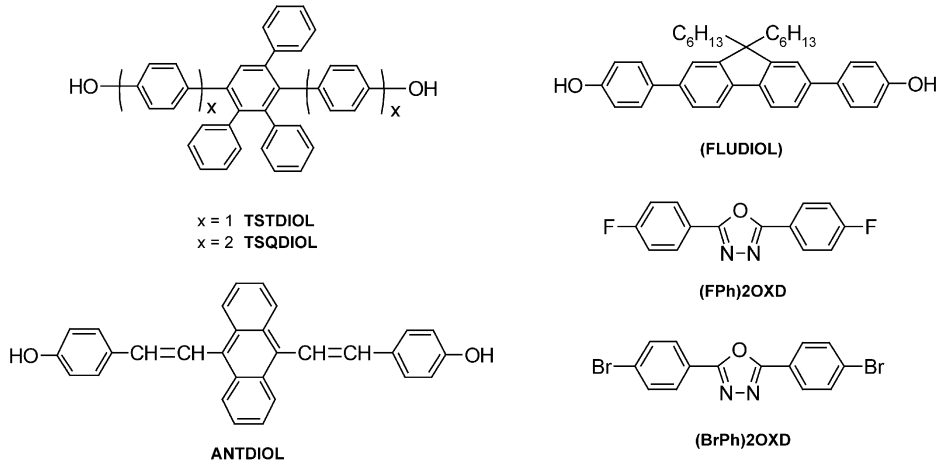


Scheme 1. Chemical structures of the monomers used for the preparation of the polymers.

### 2.2. Monomer synthesis

#### 2.2.1. 2,5-Bis(4-bromophenyl)-1,3,4-oxadiazole ((BrPh)2OXD)

To a 250 mL reaction vessel equipped with a thermometer and a magnetic stirrer was added hydrazine sulfate (1.3 g, 10 mmol), 4-bromobenzoic acid (4 g, 20 mmol) and polyphosphoric acid (40 g). The mixture was first heated slowly to 80 °C to dissolve the reactants. Then the reaction mixture was heated at 150 °C for 8 h. The mixture was further heated at cyclization temperature (200 °C) for another 2 h. After completion of the reaction, the mixture was precipitated into 150 mL of deionized water. The precipitate was recrystallized from ethanol and dried. Yield 75% (2.85 g). $^1$H NMR ($CDCl_3$, TMS): $\delta = 8.12$ (d, 4H), 7.12 (d, 4H).

#### 2.2.2. 4,4′-(9,9-Dihexyl-2,7-fluorene)-biphenol (FLUDIOL)

9,9-Dihexylfluorene-2,7-diboronic acid (2 g, 4.8 mmol), *p*-bromo-acetoxy-phenyl (2.6 g, 12 mmol) and 230 mg tetrakis(triphenylphosphine)palladium [$Pd(PPh_3)_4$] were placed together in a reaction flask. The flask was degassed and filled with argon several times. Previously, degassed toluene (50 mL) and 2 M $Na_2CO_3$ (10 mL) were added and

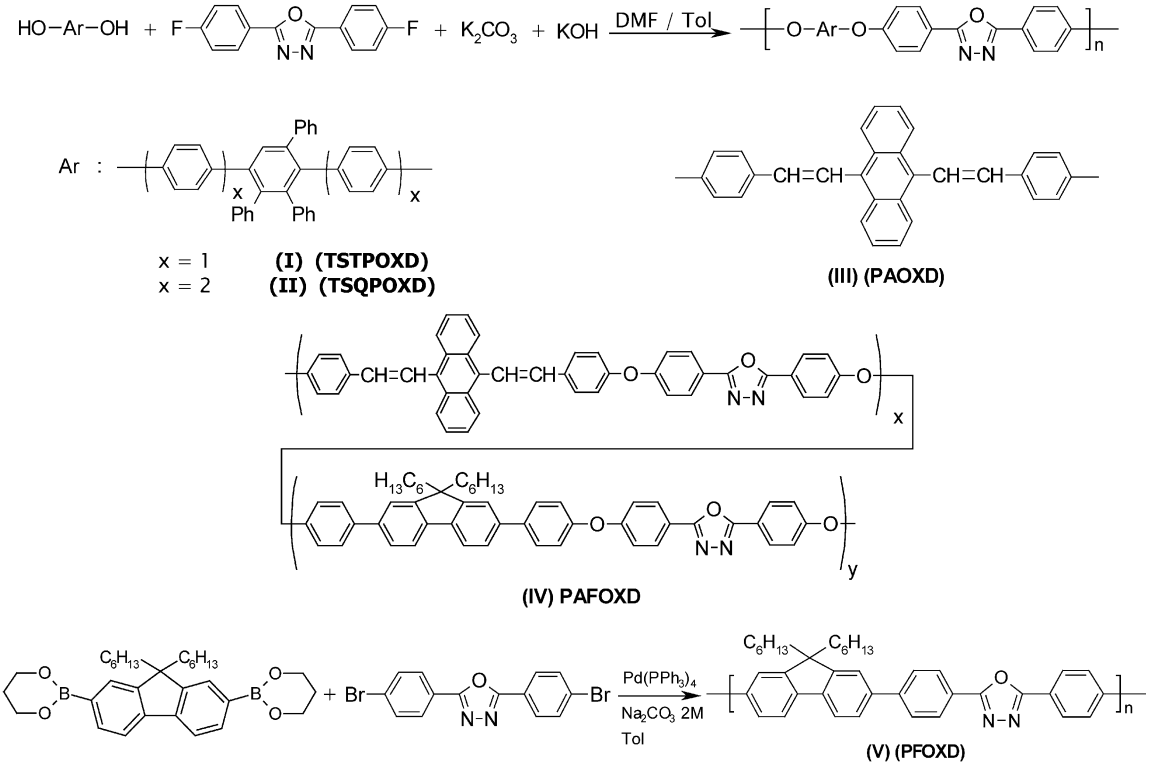


Scheme 2. Chemical structures of the synthesized copolymers.

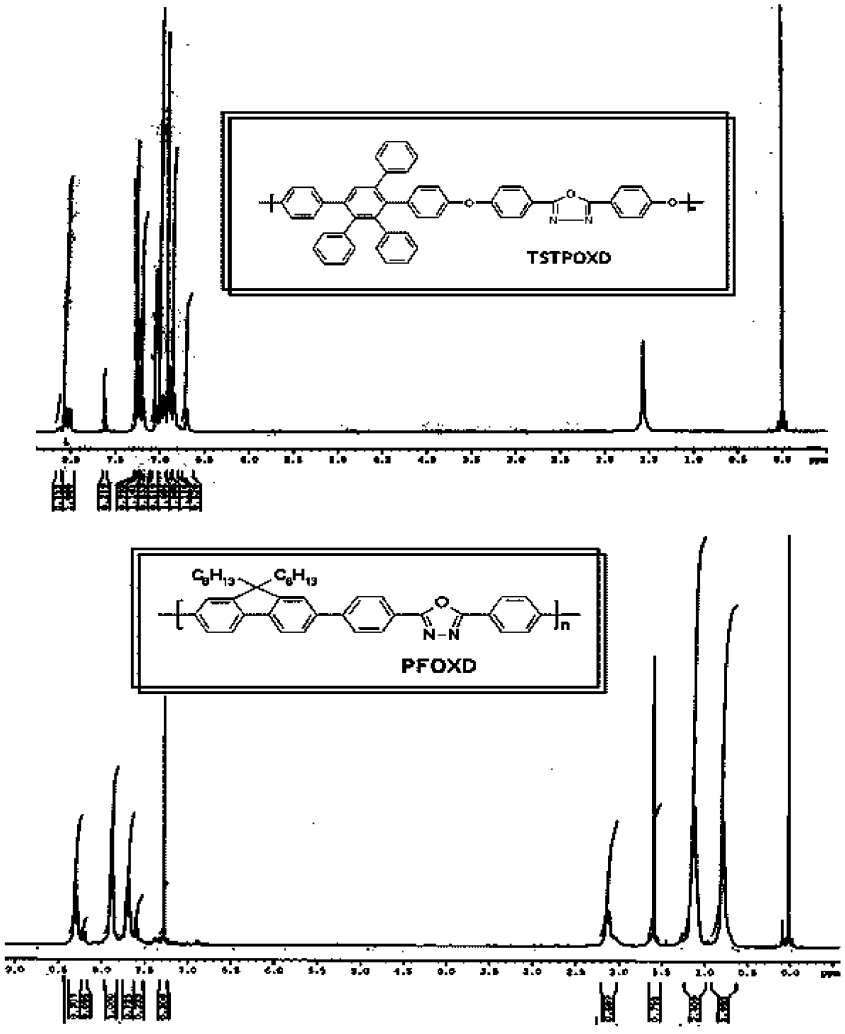


Fig. 1. $^1$H NMR spectra of the TSTPOXD and PFOXD in $CDCl_3$. The spectra are in accordance with the chemical structures of the copolymers.

the mixture was heated at reflux for 48 h. Afterwards $CHCl_3$ (50 mL) was added, and the solution was then extracted twice with water (50 mL). The combined organic layers were dried over $MgSO_4$ and the solvent was removed under reduced pressure and dried in vacuum. The crude product (2.42 g), tetrahydrofuran (50 mL) and KOH 10 N (4.02 mL, 40.2 mmol) were placed together in a reaction flask under argon atmosphere. The mixture was stirred and heated at reflux for 48 h. The resulting light-green precipitate was filtered and dissolved in MeOH. HCl 6 N (100 mL) was

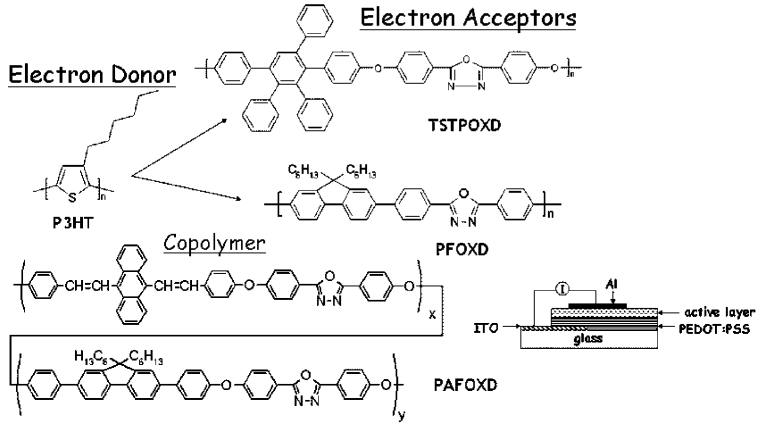


Scheme 3. Schematic representation of the device fabrication and the materials used in this study.

added at 0 °C and the mixture was stirred for 24 h. The product was isolated by filtration, washed several times with water and dried in vacuum. The crude product was purified by chromatography on silica gel column using Tol:AcOEt with ratio of 6:1 as eluent, giving 0.55 g. $^1$H NMR ($CDCl_3$, TMS): $\delta = 7.73$ (d, 2H), 7.54 (m, 8H), 6.94 (m, 4H), 2.02 (m, 4H), 1.08 (m, 16H), 0.75 (t, 6H).

### 2.3. Polymer synthesis

#### 2.3.1. General procedure for preparing oxadiazole polyethers

In a round bottomed flask a Dean-Stark trap was fitted, degassed and filled with argon three times. (FPh)2OXD (0.6024 mmol), TSTDIOL, TSQDIOL, ANTDIOL and ANTDIOL/FLUDIOL (70/30) (0.6024 mmol) were placed in the flask, respectively. Potassium carbonate (0.6928 mmol) and potassium hydroxide (1.2048 mmol) were added together and the flask was purged with argon three more times. A mixture of dimethylformamide (1.31 mL) and toluene (0.79 mL) was added and the mixture heated at 140 °C under stirring overnight. Afterwards, the temperature was increased to 180 °C and stirred for another 6 h. The reaction mixture was poured in methanol and the precipitate was filtered and washed with excess of water and methanol and dried in vacuum.

#### 2.3.2. Fluorene–oxadiazole copolymer via Suzuki coupling polymerization method

Under an argon atmosphere, 9,9-dihexylfluorene-2,7-diboronic acid (200 mg, 0.3984 mmol), 2,5-bis(4-bromophenyl)-1,3,4-oxadiazole ((BrPh)2OXD) (151.3 mg, 0.3984 mmol), $Pd(PPh_3)_4$ (23 mg, 0.020 mmol), toluene (5 mL) and 2 M $Na_2CO_3$ (1 mL) were placed in a one-necked flask and refluxed for 72 h. After cooling, the mixture was diluted with $CHCl_3$ (30 mL) and filtrated. The filtrate was washed with water and the organic layer was dried over magnesium sulfate. The solvent was evaporated to 5 mL, poured into methanol (20 fold excess of volume), and the solid precipitate formed was filtrated and washed with water, acetone and methanol. Drying over high vacuum gave 130 mg of a green pale solid.

## 3. Results and discussion

### 3.1. Preparation and solubility of the copolymers

Polymers (**I**–**IV**) were synthesized by nucleophilic substitution of the aromatic bisfluoro compound ((FPh)2OXD) with bisphenols (TSTDIOL, TSQDIOL, ANTDIOL and ANTDIOL/FLUDIOL (70/30)) as shown in Scheme 2. The polymerization procedure runs in an azeotropic mixture of the aprotic polar solvents of dimethylformamide and toluene at 140 °C for 12 h and at 180 °C for 6 h in a presence of $K_2CO_3$ and KOH as base. The molecular weights of the resulting copolymers are depicted in the Table 1. The TSTPOXD, TSQPOXD and PFOXD are soluble in common organic solvents such as tetrahydrofuran (THF), dimethylsulfoxide (DMSO), chloroform ($CHCl_3$), *o*-dichlorobenzene (ODCB), while the PAOXD is quite soluble only at 1,1,2,2-tetrachloroethane (TCE). NMR spectra of polymers TSTPOXD and PFOXD are depicted in Fig. 1. A copolymer consisting of ANTDIOL/FLUDIOL in 70/30 ratio was also synthesized and the resulting PAFOXD was soluble in ODCB and dimethylformamide (DMF). The good solubility of these polymers is in contrast to other polymers containing five member heterocyclic rings in the polymer backbone and indicates that are suitable candidates in an optoelectronic device preparation.

### 3.2. Optical properties

The absorption and emission spectral data for the polymers in solution and as thin films casting from solution in $CHCl_3$, ODCB and TCE are summarized in Table 1. The absorption spectra of the polymers obtained as thin films are shown in Fig. 2 to reveal the effects of changing the polymer backbone structure on the optical band gap and $\pi$–$\pi^*$ transition maxima ($\lambda_{max}$). All the polymers show maximum absorptions in the range of 307–415 nm in solution and in 310–422 nm as thin films. It is shown that the absorption is not changed passing from solution to the solid state except from PAFOXD which a difference of 30 nm is observed between solution and solid state. Thus, the electronic transitions of the polymers are primarily determined by their molecular structures, which are insignificantly affected by their aggregation states. Moreover, PAFOXD and PAOXD as thin deposits show two absorption bands centered at 312 and 422 nm and attributed to the $\pi$–$\pi^*$ electronic transitions of the oxadiazole and anthracene moieties, respectively. Hence, the appearance of the two well resolved absorption maxima reveals that the covalently linked anthracene and oxadiazole moieties retain the electronic properties of the separated molecules and charge transfer in the ground state does not occur [11]. The optical band gaps ($E_g$) of the polymers were estimated from the onset absorption wavelength in their UV–vis spectra in solid state to be around 3.5 eV except from the PFOXD that exhibits a value of 3.0 eV. The emission spectra of the copolymers are ranging from 380 to 425 nm in solution and in 375–568 nm as thin films. This reveals that the TSTPOXD, TSQPOXD, PFOXD are capable of producing blue light while PAOXD and PAFOXD are yellow light emitters. When PAOXD and PAFOXD are excited at 420 nm then the resulting emission peaks are centered at 568 nm with a shoulder at 600 nm. On the contrary, when PAFOXD and PAOXD are excited at 310 nm (at the absorption maxima of the oxadiazole unit) then the emission spectrum of the copolymer shows two well resolved peaks centered at 420 and 525 nm (spectra not shown). In addition,

Table 1
Molecular weights, polydispersities and UV absorption and emission characteristics of the synthesized copolymers in solution and in solid state

| Polymers | $M_n$ | $M_w$ | PDI | $\lambda_{max}$ (nm) sol | $\lambda_{max}$ (nm) film | PL (nm) sol | PL (nm) film |
|---|---|---|---|---|---|---|---|
| PAFOXD | 13,000 | 27,300 | 2.1 | 308, 392 | 314, 422 | 464 | 568, 600 |
| PAOXD | 6200 | 13,640 | 2.2 | 307, 415 | 310, 417 | 462 | 568, 600 |
| PFOXD | 3150 | 6300 | 2.0 | 362 | 362 | 405, 425 | 428, 460, 507 |
| TSTPOXD | 7230 | 18,075 | 2.5 | 270, 308 | 310 | 380 | 410, 425 |
| TSQPOXD | 18,700 | 50,490 | 2.7 | 270, 308 | 310 | 383 | 408, 513 |

Fig. 2(b) reveals that TSTPOXD is capable of producing pure blue light emission with a maximum emission peak at 415 nm. On the other hand, TSQPOXD exhibits a low energy emission band centered at 525 nm, which in this case is attributed to aggregate formation. This means that the detailed chemical structure of the TSTPOXD and TSQPOXD plays an important role on their optical properties. By adding two phenyl rings on the backbone of the chromophore unit, probably a closer packing of the chains is favorable in the solid state in the case of TSQPOXD. In polyfluorenes, a well known and examined electroluminescent polymer, one of the major problems is the appearance of a similar emission band occurring at 525–535 nm after thermal and photo-oxidation treatment which converts the blue light to an undesirable blue-green shade.

### 3.3. Photovoltaic devices

Polymer solar cells were fabricated as shown in Scheme 3 using P3HT as the electron donor and TSTPOXD or PFOXD as the electron acceptors. Furthermore, single layer devices consisted of P3HT or PAFOXD were tested. Photovoltaic cells were made by sandwiching the photoactive layer (blends of P3HT with oxadiazole copolymers in different weight ratios or single layer of PAFOXD or P3HT) between two electrodes. The composite layer was spin-coated from either a chloroform solution in the case of the polymer blends or from *o*-dichlorobenzene (ODCB) solution in the case of the PAFOXD copolymer on the surface of the anode. ITO/PEDOT:PSS is used as transparent high-work function electrode to collect the holes, whereas Al is used as low-work function electrode for electron collection. Table 2 summarises the photovoltaic characteristics of the systems tested.

#### 3.3.1. P3HT/TSTPOXD blends

Blends of various concentrations of P3HT/TSTPOXD (1/1, 1/2 and 1/4 w/w) were prepared and studied. Evidence for photo-induced electron transfer in the blend is provided by the quenching of the photoluminescence spectra of P3HT in the presence of TSTPOXD. In Fig. 3, a significant but incomplete quenching is consistent with the scale of phase separation. Therefore, some of the photogenarated electrons are transferred to the phase of the acceptor (TSTPOXD) while the others are recombined giving the characteristic emission of the P3HT. The photoluminescence spectrum of P3HT/TSTPOXD (1/2 and 1/4 w/w) are blue shifted relative of the spectrum of the neat film of P3HT and to the spectrum of P3HT/TSTPOXD (1/1 w/w). Blue shifted polymer emission caused by the presence of other acceptors such as fullerenes or polymers has previously been observed [12].

The influence of the solvent on the morphology of the spin-coated layer is depicted in Fig. 4(a) and (b). Both AFM images show the morphology of the P3HT/TSTPOXD (1/2 w/w) blend that was spin-coated using either (a) chloroform or (b) ODCB. It can be seen that the scale of the phase

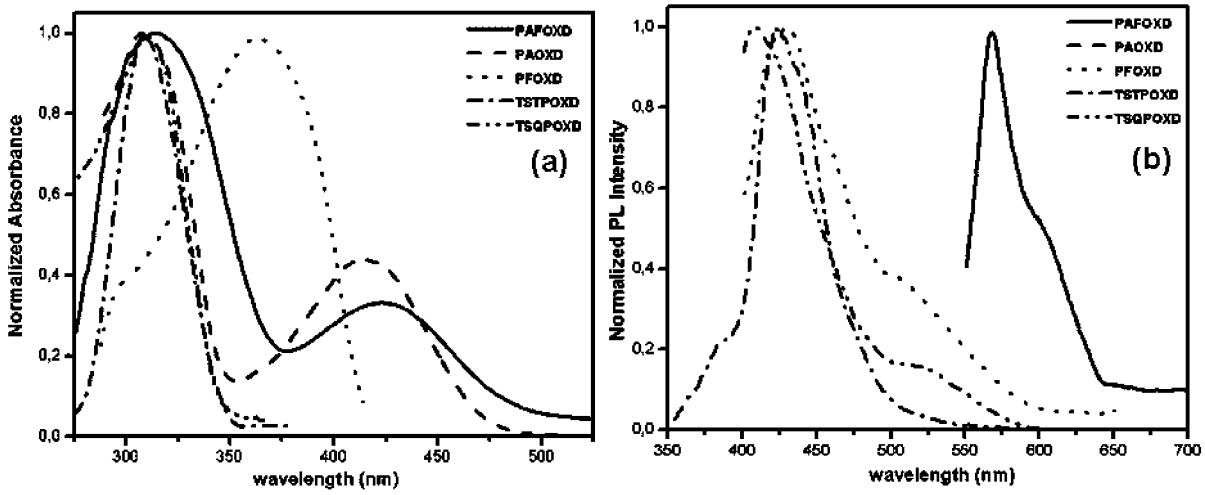


Fig. 2. (a) UV absorption spectra of the synthesized copolymers in chloroform and ODCB solutions. (b) Photoluminescence spectra of the TSTPOXD, TSQPOXD excitation wavelength was 310 nm, PFOXD with excitation wavelength at 360 nm and PAOXD and PAFOXD excited at 420 nm.

Table 2
Photovoltaic performance characteristics; open-circuit voltages ($V_{oc}$), fill factors (FF) and power conversion efficiencies for all the examined systems

| Active layer | Open-circuit voltage (V) | Fill factor (FF) | Power conversion efficiency ($\times 10^{-3}$%) |
|---|---|---|---|
| P3HT/TSTPOXD (1/2 w/w) | 0.65 | 0.17 | 0.31 |
| P3HT/PFOXD (1/2 w/w) | 0.46 | 0.24 | 0.48 |
| PAFOXD | 0.89 | 0.18 | 0.036 |

separation of the film prepared from the chloroform solution is much finer than the phase separation of the film prepared by spin-coating the same blend from ODCB. Based on Fig. 4(a), the size of the phase separation is in the range of 200–400 nm when chloroform is used as solvent, while domains in the order of 1700–1800 nm are observed in the case when ODCB is used. The differences in Fig. 4(a) and (b) are due to the rapid solvent evaporation occurring during the spin-coating of the blend from chloroform solution in ambient conditions. This prevents significant rearrangement of the polymer chains and quenches a fine phase separation, as shown in Fig. 4(a). Unfortunately, due to the low power conversion efficiencies of the photocells fabricated from chloroform and ODCB solutions of P3HT/TSTPOXD (1/2 w/w) blend, correlation between the two morphologies observed above and the photovoltaic behavior of the devices is not possible.

In a similar study, blends of P3HT/PFOXD in different weight ratios were also examined focusing on the photo-induced electron transfer from the photoluminescence quenching and the surface morphology from the AFM measurements. The results are similar to that of the previous blend tested (P3HT/TSTPOXD) and depicted in Fig. 5.

### 3.3.2. PAFOXD copolymer

The morphological study for PAFOXD was performed using the AFM technique. The study of the surface morphology of the copolymer as thin deposit spin-coated from *o*-dichlorobenzene solution reveals the formation of continuous pathways as shown in Fig. 6. More specifically, a string-like morphology is observed in the $5\times5$ μm$^2$ picture of Fig. 6. This string-like morphology resembles a bicontinuous network in the range of 220 nm that favors charge transport and the subsequently collection of holes and electrons at the preferred electrodes.

The current–voltage (*I–V*) characteristics of ITO/PEDOT-PSS/PAFOXD/Al device with an active area of 0.04 cm$^2$ in the dark and under irradiation with white light of 50 mW cm$^{-2}$ are presented in Fig. 7. Illumination from the ITO side produced a clear photovoltaic behavior. In particular, a short-circuit current $I_{sc}=0.11$ μA/cm$^2$ and an open-circuit voltage of $V_{oc}=0.89$ V were obtained.

Based on the simple model of a metal–insulator–metal (MIM) diode [13] and assuming both contacts to be neutral, one would expect the saturated open-circuit voltage to be approximately equal to the difference of the work functions of the two electrodes. Unlike the value of the Al work function, which is well accepted to be 4.3 eV, the value for a standard PEDOT/PSS layer is uncertain; according to published results, it is around 5.2 eV [14,15]. Therefore, our measured open-circuit voltage correspond to the MIM model prediction. Despite the low energy conversion

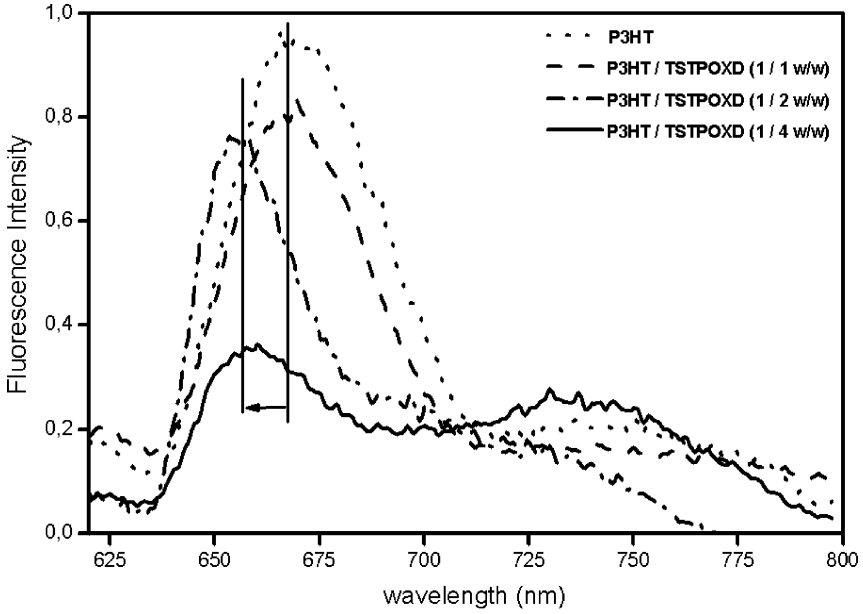


Fig. 3. Photoluminescence spectra of P3HT and P3HT/TSTPOXD mixtures in different weight ratios.

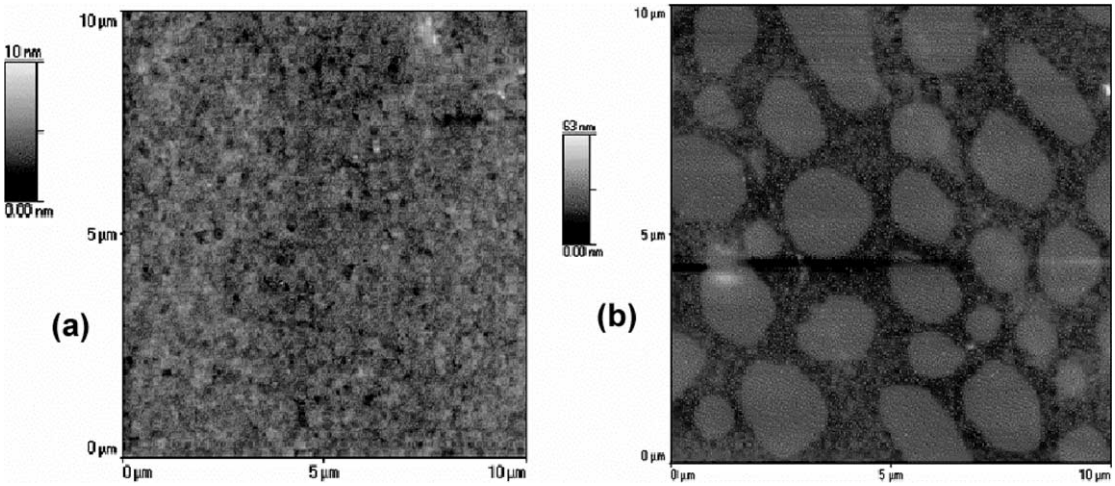


Fig. 4. AFM micrographs showing the change of the surface morphology of the P3HT/TSTPOXD (1/2 w/w) blend that was spin-coated using (a) chloroform and (b) ODCB.

efficiency of the copolymer, the extremely high open-circuit voltage (0.89 V) which is very close to the upper limit of $V_{oc}$ of the device based on the MIM model makes the copolymer approach and this material in particular a promising candidate for the application in photovoltaic organic cells. This value of $V_{oc}$ obtained from PAFOXD is one of the highest reported in the literature involving copolymers [10, 16]. However, comparable or higher values have been reported for other donor–acceptor copolymers [17]. On the other hand, the reason for the low power efficiency is that

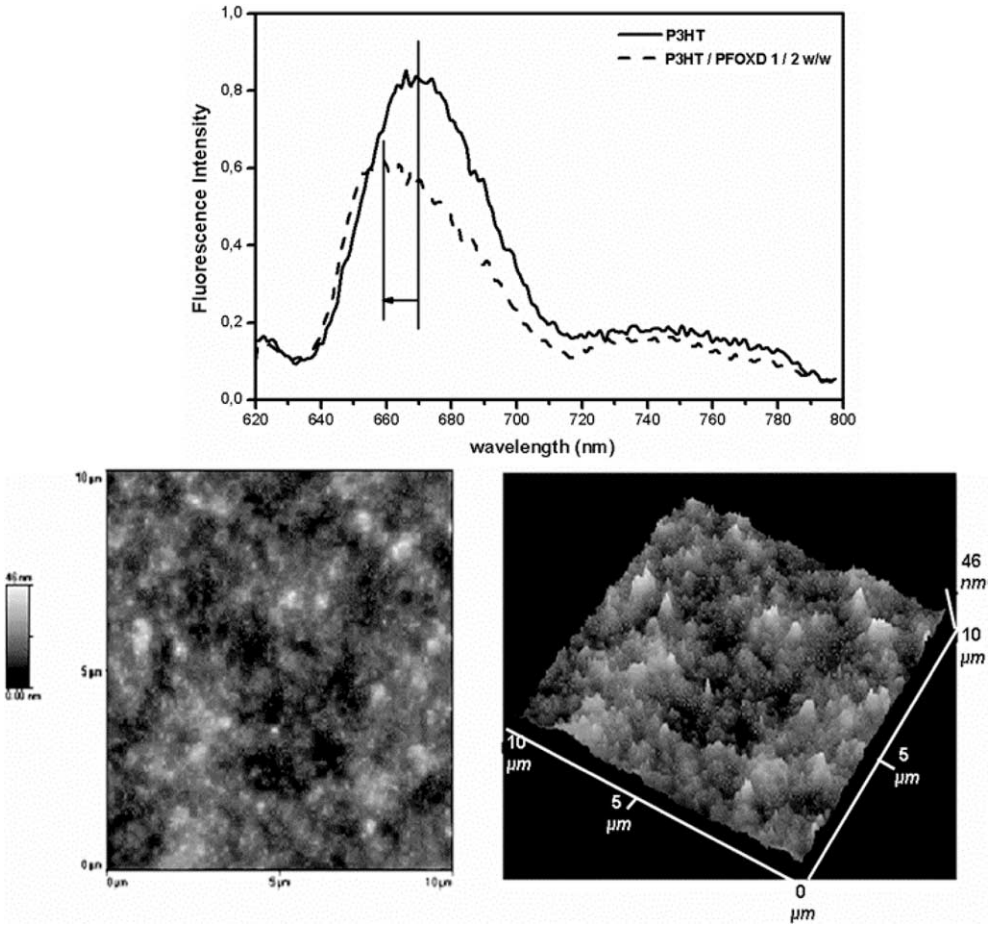


Fig. 5. Photoluminescence spectra of P3HT and P3HT/PFOXD mixtures in different weight ratios. AFM micrographs showing the surface morphology of the P3HT/PFOXD (1/2 w/w) blend that was spin-coated from a chloroform solution.

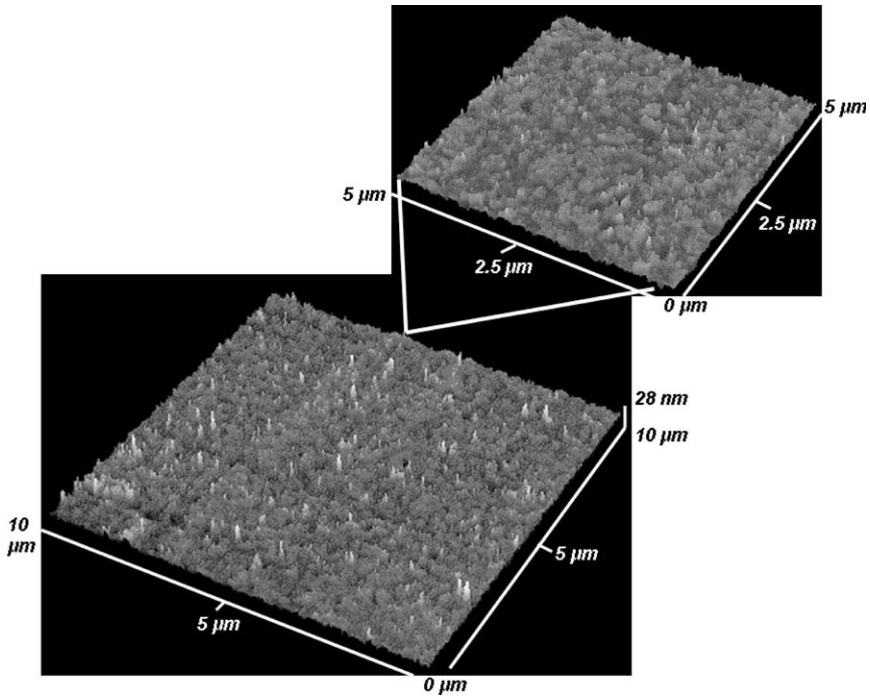


Fig. 6. Three-dimensional AFM rendering micrographs ($10\times10$ and $5\times5$ $\mu m^2$) of the surface pattern formed by the PAFOXD on glass substrate.

the copolymer exhibits a very low short-circuit current $I_{sc}$ due to the fact that the anthracene unit in the polymer backbone is not a strong absorber of sun light (does not absorb in the red part of the terrestrial spectrum 600–800 nm). Enhancement of the conversion efficiency of the device could be achieved by the addition of a proper organic dye, which would absorb in the red region of the solar spectrum. Furthermore, we note that processing of the photoactive layer and the *I–V* characterization of the device was done in a normal lab atmosphere without protection from oxygen. This most likely affects negatively the energy conversion efficiency of the device and we are confident that the performance of PAFOXD devices can be dramatically improved in conditions where oxygen and moisture are excluded.

## 4. Conclusions

New copoly(arylethers) containing 1,3,4-oxadiazole units in the main chain were synthesized. These polymers are soluble in common organic solvents. Blends from those polymers with P3HT were prepared and investigated with optical and AFM techniques. All the prepared mixtures

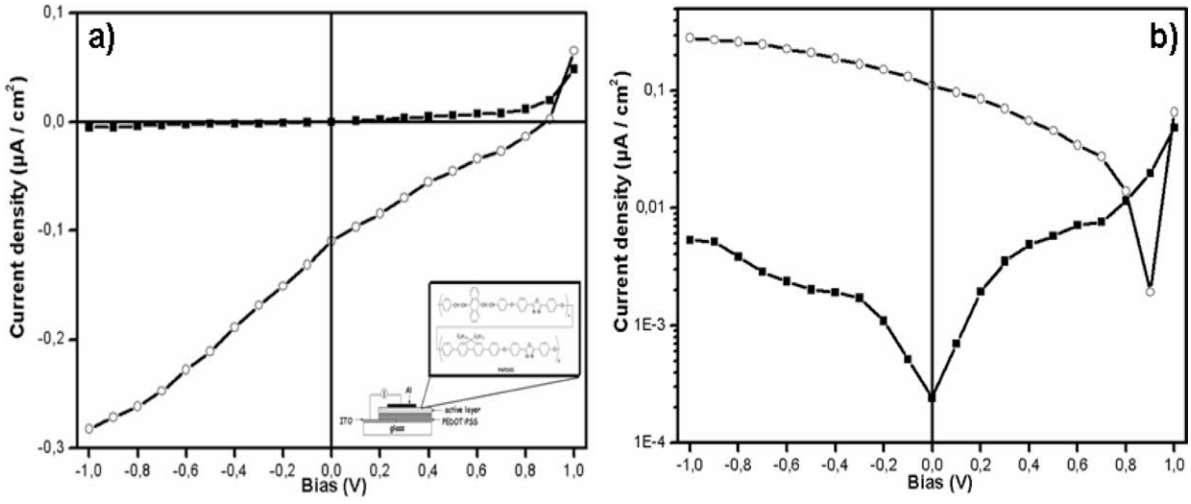


Fig. 7. *I–V* curves of an ITO/PEDOT:PSS/PAFOXD/Al device in the dark (solid squares) and under white-light illumination (open holes) (a) linear plot and (b) semi-log plot.

made by P3HT and TSTPOXD or PFOXD showed photoluminescence quenching compared to the emission spectra of P3HT. This finding confirms a charge transfer from the phase of the electron donor (P3HT) to the phase of the electron acceptor. The thin film morphology is significantly influenced by the solvent used resulting in a phase separation in the nanometer scale. In more detail, for P3HT/TSTPOXD it was shown that when $CHCl_3$ was used as solvent instead of ODCB a much finer phase separation was appeared which is preferable for photovoltaic applications. Finally, photocells made by the P3HT/TSTPOXD or PFOXD blends and a single layer device consisted of PAFOXD were examined for their photovoltaic response. Despite the low power conversion efficiencies achieved, in the case of PAFOXD a very high open-circuit voltage (0.89 V) was observed which is one of the highest reported in the literature involving a copolymer showing the promise of the copolymer approach in the fabrication of polymeric photovoltaic devices.

## Acknowledgements

The authors are grateful to Konarka Technologies of Lowell, MA, USA and the Greek Ministry of Development, under the grant EPAN E13 for the financial support of the project. In addition, we would like to thank Dr Russell Gaudiana of Konarka Technologies for the helpful discussions. Finally, we also thank Dr Vasilis Dracopoulos of FORTH-ICEHT for the help in acquiring the AFM images.

## References

[1] Brabec CJ, Hummelen JC, Sariciftci SN. Adv Funct Mater 2001;11:15.
[2] (a) Wienk MM, Kroon JM, Verhees WJH, Knol J, Hummelen JC, Van Hal PA, et al. Angew Chem Int Ed 2003;42:3371.
(b) Padinger F, Rittberger R, Sariciftci NS. Adv Funct Mater 2003;13:85.
[3] Ouali L, Krasnikov VV, Stalmach U, Hadziioannou G. Adv Mater 1999;11:1515.
[4] (a) Lee JK, Klaerner G, Miller RD. Chem Mater 1999;11:1083.
(b) Cui Y, Zhang X, Jenekhe SA. Macromolecules 1999;32:3824.
(c) Yamamoto T, Sugiyama K, Kushida T, Inoue T, Kanbara T. J Am Chem Soc 1996;118:3930.
(d) Zhang X, Shetty AS, Jenekhe SA. Macromolecules 1999;32:7422.
(e) Dai Y, Katz TJ. J Organomet Chem 1997;62:1274.
[5] (a) Jenekhe SA, Chen XL. J Phys Chem B 2000;104:6332.
(b) Huang WY, Yun H, Lin HS, Kwei TK, Okamoto Y. Macromolecules 1999;32:8089.
(c) Lu L, Jenekhe SA. Macromolecules 2001;34:6249.
(d) Chiang CL, Shu CF. Chem Mater 2002;14:682.
(e) Zhang X, Kale DM, Jenekhe SA. Macromolecules 2002;35:382.
[6] (a) Strukelj M, Papadimitrakopoulos F, Miller TM, Rothberg LJ. Science 1995;267:1969.
(b) Cacialli F, Li X, Friend RH, Moratti SC, Holmes AB. Synth Met 1995;75:161.
(c) Li XC, Cacialli F, Gilles M, Grüner J, Friend RH, Holmes AB, et al. Adv Mater 1995;7:898.
(d) Ueda M, Oda M. Polym J 1989;21:193.
[7] (a) Schulz B, Bruma M, Brehmer L. Adv Mater 1997;9:601.
(b) Huang W, Meng H, Yu WL, Pei J, Chen ZK, Lai YH. Macromolecules 1999;32:118.
(c) Peng Z, Bao M, Galvin ME. Chem Mater 1998;10:2086.
[8] (a) Tsutsui T, Aminaka EI, Fujita Y, Hamada Y, Saito S. Synth Met 1993;55–57:4157.
(b) Tsutsui T. MRS Bull 1997;22:39.
(c) Hamada Y, Adachi C, Tsutsui T, Saito S. Jpn J Appl Phys 1992;31:1812.
[9] Kulkarni AP, Tonzola CJ, Babel A, Jenekhe SA. Chem Mater 2004;16:4556.
[10] (a) Konstandakopoulou FD, Kallitsis JK. J Polym Sci, Part A: Polym Chem 1999;37:3826.
(b) Kakali F, Gravalos KG, Kallitsis JK. J Polym Sci, Part A: Polym Chem 1996;34:1581.
(c) Tsai CJ, Chen Y. J Polym Sci, Part A: Polym Chem 2002;40:293.
[11] Peeters E, van Hal PA, Knol J, Brabec CJ, Sariciftci NS, Hummelen JC, et al. J Phys Chem B 2000;104:10174.
[12] (a) Sariciftci NS, Smilowitz L, Heeger AJ, Wudl F. Science 1992;258:1474.
(b) Jenekhe SA, Paor LR, Chen XL, Tarkka RM. Chem Mater 1996;8:2401.
(c) Lee SB, Zakhidov AA, Khairullin II, Sokolov VY, Khabibullaev PK, Tada K, et al. Synth Met 1996;77:155.
(d) Hasharoni K, Keshavarz M, Sastre A, Gonzales A, Bellavia-Lund C, Greewald Y, et al. J Chem Phys 1997;107:2308.
(e) Theander M, Yartsev A, Zigmantas D, Sundström V, Mammo W, Andersson MR, et al. Phys Rev B 2000;61:12957.
[13] Parker ID. J Appl Phys 1994;75:1656.
[14] Xing KZ, Fahlman M, Chen XW, Inganas O, Salaneck WR. Synth Met 1997;89:161.
[15] Kim JS, Granstrom M, Friend RH, Johanssen N, Salaneck WR, Daik R, et al. J Appl Phys 1998;84:6859.
[16] (a) Eckert JF, Nicoud JF, Nierengarten JF, Liu SG, Echegoyen L, Barigelletti F, et al. J Am Chem Soc 2000;122:7467.
(b) Ramos AM, Rispens MT, van Duren JKJ, Hummelen JC, Janssen RAJ. J Am Chem Soc 2001;123:6714.
(c) Gu T, Tsamouras D, Melzer C, Krasnikov V, Gisselbrecht JP, Gross M, et al. Chem Phys Chem 2002;1:124.
[17] Jenekhe SA, Lu L, Alam MM. Macromolecules 2001;34:7315.